(Received 16 April 2025, Accepted 18 July 2025, Scheduled 31 July 2025)

Fundamental GDOP Bounds and Base Station Deployment in 2D TDOA Positioning Systems

Shaohan Feng[1,2], Weiguang Shi[1,2,*], Yongtao Ma[3], Wanru Ning[4], and Zihang Meng[5]

[1]School of Electronics and Information Engineering, Tiangong University, Tianjin 300387, China
[2]Tianjin Key Laboratory of Optoelectronic Detection Technology and Systems, Tianjin 300387, China
[3]School of Microelectronics, Tianjin University, Tianjin 300072, China
[4]School of Computer Science, Peking University, Beijing 100871, China
[5]School of Astronautics, Harbin Institute of Technology, Harbin 150000, China

ABSTRACT: This paper investigates the theoretical bounds of geometric dilution of precision (GDOP) in two-dimensional time difference of arrival (TDOA) positioning systems. The corresponding base station (BS) deployment for a single mobile terminal (MT) is subsequently derived. Considering the correlation of time difference measurements, a simplified closed-form expression for GDOP is first derived, and it is shown that GDOP is independent of the selection of the reference BS. Theoretical bounds for GDOP are rigorously established, along with the conditions under which these bounds are valid. Based on these boundary conditions, the study demonstrates that optimal deployment occurs when BSs are grouped, and the azimuths of BSs within each group are evenly distributed around a circle centered at the MT. For systems with up to five BSs, the optimal deployment is proven to be unique, whereas non-unique solutions emerge for larger configurations. In contrast, the complete solution set for the worst-case deployment occurs when BSs are collinear and symmetrically aligned along a specific coordinate origin or axis. Numerical simulations validate the theoretical findings, highlighting the superiority of uniform angular distributions. These results provide actionable guidelines for enhancing positioning accuracy in cellular networks and a foundational framework for multi-BS deployment optimization.

1. INTRODUCTION

With the advent of the mobile internet era, cellular positioning has become an integral component of mobile communication systems, supporting a wide range of services such as real-time navigation [1], security monitoring [2], logistics management [3], and geofencing [4]. In cellular positioning systems, the geometric relationship between base stations (BSs) and mobile terminals (MTs) is a critical factor affecting positioning accuracy. The geometric dilution of precision (GDOP) which is based on the Cramer-Rao lower bound (CRLB) [5] is commonly employed to evaluate the influence of this geometric relationship on positioning accuracy [6]. A lower GDOP value signifies a more favorable geometric configuration, resulting in enhanced positioning accuracy for MTs, and vice versa [7]. Moreover, the theoretical bounds of GDOP and the ideal multi-BS deployment strategies under known MT positions have attracted considerable interest within the research community [6–14].

Measuring the signal propagation time between the MT and BS is a key component of cellular positioning, with existing methods primarily relying on time of arrival (TOA) and time difference of arrival (TDOA). Unlike TOA, which relies on arrival time measurements, TDOA uses the time difference as the measurement and thus does not require strict clock synchronization between the BSs and MT, making it more widely adopted in practical applications. For TOA, it has been demonstrated that the GDOP lower bound and the corresponding optimal deployment of the BSs occur when all BSs are positioned at the vertices of a regular polygon, with the MT located at the center [8]. However, in TDOA, determining the GDOP bounds and the corresponding BS deployment is challenging, primarily due to the introduction of the reference BS concept, which causes the time difference measurements to be correlated, thereby increasing the complexity of the GDOP calculation. Paper [9] expresses GDOP using the least squares (LS) estimation method, which offers computational simplicity. However, this is an approximate solution for GDOP and is inaccurate. Since the variance of positioning results obtained with the LS method exceeds the CRLB [7], the GDOP expressed via LS is higher than the rigorous CRLB-based GDOP. Some studies assume that the time difference measurements in TDOA are uncorrelated to simplify the GDOP calculation, but this assumption is unrealistic [10–12]. On the other hand, some research on TDOA systems better reflects practical scenarios by incorporating the correlations in the time difference measurements into the model. Paper [13] analyzes the impact of measurement value correlations on GDOP, while [14] uses a heuristic optimization algorithm to study the optimal BS deployment for minimizing the GDOP. However, both of these studies lack rigorous theoretical derivation. Furthermore, paper [5] theoretically proves the optimal sensor deployment for minimizing the CRLB, while paper [15] theoretically demonstrates the optimal sensor deployment for maximizing the Fisher informa-

* Corresponding author: Weiguang Shi (shiweiguang@tiangong.edu.cn).

tion matrix (FIM). Given that CRLB, FIM, and GDOP share inherent similarities, the findings in [5, 15] provide valuable insights into the lower bound of GDOP and the corresponding optimal BS deployment. However, the analytical approaches in these two papers are relatively complex, and they do not thoroughly discuss the unique characteristics of the optimal deployment. Moreover, all the aforementioned studies [5, 9–15] offer no guidance on the upper bound of GDOP or the worst-case deployment. In contrast, this paper adopts a more intuitive and concise method by simplifying the GDOP expression and analyzing its structural form to obtain the GDOP bounds and the conditions under which these bounds hold. Based on the conditions for the bounds to hold, the optimal and worst-case BS deployments are correspondingly given, and additional theoretical analysis is performed to prove the unique characteristics of the proposed BS deployment scheme.

In summary, the contributions of this work are as follows:

1) We obtain a simplified GDOP expression considering the correlation of time difference measurements. The conclusion that the GDOP value is independent of the choice of reference BS for a given TDOA system geometry can be directly derived from the simplified GDOP expression.
2) We derive the lower bound of the GDOP value and the corresponding optimal BS deployment strategy using a clearer and simpler method. Using rigorous and consistent mathematical methods, we prove the uniqueness of the optimal BS geometric configuration for up to five BSs, while also emphasizing the non-uniqueness that arises when the number of BSs exceeds five.
3) We derive the upper bound of the GDOP value and the complete solution set for worst-case BS deployment strategy.

Numerical simulations validate the theoretical findings in the two-dimensional TDOA system and investigate the applicability of the proposed BS deployment strategy to other positioning systems, including two-dimensional TOA and direction of arrival (DOA). We anticipate that the derived lower and upper bounds on GDOP, along with the corresponding deployment strategies proposed in this study, will significantly improve the accuracy of cellular positioning systems.

2. GDOP IN TDOA POSITIONING SYSTEM

Consider a two-dimensional TDOA positioning system that consists of a single MT and N BSs where $N \geq 3$, as illustrated in Fig. 1. Let $\boldsymbol{\theta} = [x, y]^T$ implies the position of MT. $[x_n, y_n]^T$ represents the position of the nth measurement BS, with $n \in [1, N]$. Without loss of generality, let $[x_1, y_1]^T$ represent the position of reference BS. The observation vector $\boldsymbol{\Lambda}$ is formulated as $\begin{bmatrix} \Delta d_2 & \Delta d_3 & \cdots & \Delta d_N \end{bmatrix}$ with $\Delta d_n = c\Delta t_n = d_1 - d_n + e_n$, where c is the speed of light; Δt_n stands for the time difference measurement; $d_1 = \sqrt{(x-x_1)^2 + (y-y_1)^2}$; and $d_n = \sqrt{(x-x_n)^2 + (y-y_n)^2}$. e_n denotes a ranging error that follows a Gaussian distribution with zero mean, and σ is the root-mean-square error.

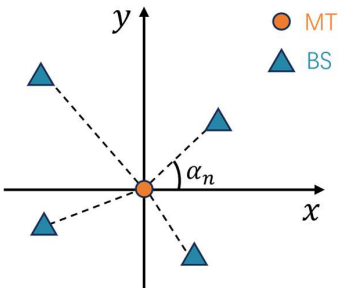

FIGURE 1. Geometry of single MT and multiple BSs.

Utilizing the best linear unbiased estimator (BLUE), the covariance for estimated value $\widehat{\boldsymbol{\theta}}$ of $\boldsymbol{\theta}$ can be calculated by

$$\mathrm{var}(\widehat{\boldsymbol{\theta}}) = \mathrm{diag}\left(\mathbf{H}^T\mathbf{Q}^{-1}\mathbf{H}\right)^{-1}, \tag{1}$$

where $\mathbf{H}$ and $\mathbf{Q}$ are the Jacobian matrix and covariance matrix referring to $\boldsymbol{\Lambda}$. According to the conclusion in [16], the CRLB of the positioning error can be determined by (1). Further, the GDOP, which serves as a convenient metric based on CRLB, is defined by [16]

$$\mathrm{GDOP} = \sqrt{\mathbf{G}_{11} + \mathbf{G}_{22}}, \tag{2}$$

with

$$\mathbf{G} = \frac{1}{\sigma^2}\left(\mathbf{H}^T\mathbf{Q}^{-1}\mathbf{H}\right)^{-1}, \tag{3}$$

where $\mathbf{G}_{11}$ and $\mathbf{G}_{22}$ are the diagonal elements of $\mathbf{G}$ matrix.

For TDOA system, $\mathbf{H}$ can be expressed as:

$$\mathbf{H}_{\mathrm{TDOA}} = \begin{bmatrix} \cos\alpha_1 - \cos\alpha_2 & \sin\alpha_1 - \sin\alpha_2 \\ \vdots & \vdots \\ \cos\alpha_1 - \cos\alpha_N & \sin\alpha_1 - \sin\alpha_N \end{bmatrix}, \tag{4}$$

where $\alpha_n \in [0, 2\pi]$ is the angle between the vector from the MT to the nth measurement BS and the positive X-axis. α_1 denotes the angle referring to the reference BS. If we directly assume that each Δd_n is uncorrelated, it will result in $\mathbf{Q}_{\mathrm{TDOA}}$ being an identity matrix, which will simplify the $\mathbf{G}$ matrix to $(\mathbf{H}^T\mathbf{H})^{-1}/\sigma^2$. However, since each Δd_n includes d_1, all these Δd_n are interdependent. Under this condition, the covariance matrix $\mathbf{Q}_{\mathrm{TDOA}}$ is defined by

$$\mathbf{Q}_{\mathrm{TDOA}} = \sigma^2 \begin{bmatrix} 2 & 1 & \cdots & 1 \\ 1 & 2 & \cdots & 1 \\ \vdots & \vdots & \ddots & \vdots \\ 1 & \cdots & 1 & 2 \end{bmatrix}_{N-1}, \tag{5}$$

and its inverse $\mathbf{Q}^{-1}_{\mathrm{TDOA}}$ is accordingly given by

$$\mathbf{Q}^{-1}_{\mathrm{TDOA}} = \frac{1}{\sigma^2} \begin{bmatrix} 1-\frac{1}{N} & -\frac{1}{N} & \cdots & -\frac{1}{N} \\ -\frac{1}{N} & 1-\frac{1}{N} & \cdots & -\frac{1}{N} \\ \vdots & \vdots & \ddots & \vdots \\ -\frac{1}{N} & -\frac{1}{N} & \cdots & 1-\frac{1}{N} \end{bmatrix}_{N-1}. \tag{6}$$

Substituting (4) and (6) into (2), the GDOP for TDOA positioning system is expressed as (7).

$$\mathrm{GDOP}=\sqrt{\frac{\sum_{n=2}^{N}\left((\cos\alpha_1-\cos\alpha_n)^2+(\sin\alpha_1-\sin\alpha_n)^2\right)-\frac{1}{N}\left(\left(\sum_{n=2}^{N}(\cos\alpha_1-\cos\alpha_n)\right)^2+\left(\sum_{n=2}^{N}(\sin\alpha_1-\sin\alpha_n)\right)^2\right)}{\left(\begin{array}{l}\left(\sum_{n=2}^{N}(\cos\alpha_1-\cos\alpha_n)^2-\frac{1}{N}\left(\sum_{n=2}^{N}(\cos\alpha_1-\cos\alpha_n)\right)^2\right)\left(\sum_{n=2}^{N}(\sin\alpha_1-\sin\alpha_n)^2-\frac{1}{N}\left(\sum_{n=2}^{N}(\sin\alpha_1-\sin\alpha_n)\right)^2\right)\\ -\left(\sum_{n=2}^{N}(\cos\alpha_1-\cos\alpha_n)(\sin\alpha_1-\sin\alpha_n)-\frac{1}{N}\sum_{n=2}^{N}(\cos\alpha_1-\cos\alpha_n)\sum_{n=2}^{N}(\sin\alpha_1-\sin\alpha_n)\right)^2\end{array}\right)}}. \tag{7}$$

3. METHODOLOGY

3.1. Primary

As shown in (7), the value of GDOP is influenced by the azimuths of all BSs. To facilitate the analysis of this influence, we make the following substitutions and simplifications:

$$\begin{aligned}A &= \sum_{n=2}^{N}(\cos\alpha_1-\cos\alpha_n)^2-\frac{1}{N}\left(\sum_{n=2}^{N}(\cos\alpha_1-\cos\alpha_n)\right)^2\\ &= \sum_{n=1}^{N}\cos^2\alpha_n-\frac{1}{N}\left(\sum_{n=1}^{N}\cos\alpha_n\right)^2=N\mathrm{var}(\cos\alpha_n), \quad (8)\\ B &= \sum_{n=2}^{N}(\sin\alpha_1-\sin\alpha_n)^2-\frac{1}{N}\left(\sum_{n=2}^{N}(\sin\alpha_1-\sin\alpha_n)\right)^2\\ &= \sum_{n=1}^{N}\sin^2\alpha_n-\frac{1}{N}\left(\sum_{n=1}^{N}\sin\alpha_n\right)^2=N\mathrm{var}(\sin\alpha_n), \quad (9)\\ C &= \sum_{n=2}^{N}(\cos\alpha_1-\cos\alpha_n)(\sin\alpha_1-\sin\alpha_n)\\ &\quad -\frac{1}{N}\sum_{n=2}^{N}(\cos\alpha_1-\cos\alpha_n)\sum_{n=2}^{N}(\sin\alpha_1-\sin\alpha_n)\\ &= \sum_{n=1}^{N}\cos\alpha_n\sin\alpha_n-\frac{1}{N}\sum_{n=1}^{N}\cos\alpha_n\sum_{n=1}^{N}\sin\alpha_n\\ &= N\mathrm{cov}(\cos\alpha_n,\sin\alpha_n), \quad (10)\end{aligned}$$

where var and cov represent variance and covariance operations, respectively. Subsequently, (7) is simplified to:

$$\mathrm{GDOP}_{\mathrm{TDOA}}=\sqrt{\frac{A+B}{AB-C^2}}. \tag{11}$$

Equation (11) is a simplified GDOP expression. Based on this, a proposition is obtained for the relationship between GDOP and the choice of reference BS.

Proposition 1. For TDOA positioning system, the value of GDOP is independent of the choice of reference BS.

Proof. The difference terms $\cos\alpha_1-\cos\alpha_n$ and $\sin\alpha_1-\sin\alpha_n$ in (7) seem to indicate that the selection of the reference BS has some impact on the GDOP. However, the simplified GDOP expression contains terms of A, B, and C which only depend respectively on the variance of $\cos\alpha_n$, the variance of $\sin\alpha_n$, and the covariance between them. Therefore, for a given set of BS azimuths, the GDOP remains unchanged regardless of which BS is chosen as the reference.

3.2. The Lowest GDOP Value and Its Conditions

Since A and B are determined by the product of N times the variance terms, $A\geq 0$ and $B\geq 0$ are established. The equality holds if and only if $\cos\alpha_1=\cos\alpha_2=\cdots=\cos\alpha_N$ or $\sin\alpha_1=\sin\alpha_2=\cdots=\sin\alpha_N$. However, if either of these equalities holds, it leads to $C=0$, $AB=0$, and $A+B>0$, which results in an infinite GDOP value (this issue will be discussed in detail in Section 3.5). Furthermore, if both conditions hold simultaneously, the matrix $\mathbf{G}$ cannot be computed due to $\mathbf{H}_{\mathrm{TDOA}}=\mathbf{0}$, i.e., at this point, (11) represents a degenerate case of $0/0$. This ensures that $A>0$ and $B>0$ are always satisfied when minimizing GDOP. Based on this, by dividing the numerator and denominator in the square root of (11) by $A+B$, (11) is updated as:

$$\mathrm{GDOP}_{\mathrm{TDOA}}=\sqrt{\frac{1}{D-E}}, \tag{12}$$

with

$$D = \frac{1}{\frac{1}{A}+\frac{1}{B}}, \tag{13}$$

$$E = \frac{C^2}{A+B}. \tag{14}$$

According to (12), maximizing D and minimizing E simultaneously leads to a minimum GDOP value.

1) Observations on D

According to arithmetic mean-quadratic mean inequality, we have

$$2D=\frac{2}{\frac{1}{A}+\frac{1}{B}}\leq\frac{A+B}{2}. \tag{15}$$

The equal sign holds if and only if $A=B$. Meanwhile, $A+B$ can be simplified as

$$A+B=N-\frac{1}{N}\left(\left(\sum_{n=1}^{N}\cos\alpha_n\right)^2+\left(\sum_{n=1}^{N}\sin\alpha_n\right)^2\right). \tag{16}$$

It is clear that $\max(A+B)=N$ occurs only when $\sum_{n=1}^{N}\cos\alpha_n=0$ and $\sum_{n=1}^{N}\sin\alpha_n=0$. Accordingly, we have $\max(D)=N/4$ based on (15). Under the conditions $\sum_{n=1}^{N}\cos\alpha_n=0$ and $\sum_{n=1}^{N}\sin\alpha_n=0$, and considering $A=B$, $\sum_{n=1}^{N}\cos 2\alpha_n=0$ is obtained.

2) Observations on E

Noticing that $A+B \geq 0$ and since the numerator of E is the square of a number, it follows that $E \geq 0$. Hence, $\min(E) = 0$ occurs when $C = 0$. Under the condition $C = 0$ and considering $\sum_{n=1}^{N} \cos\alpha_n = 0$ and $\sum_{n=1}^{N} \sin\alpha_n = 0$, $\sum_{n=1}^{N} \sin 2\alpha_n = 0$ is then deduced.

3) Minimum GDOP

By simultaneously maximizing D and minimizing E, the minimum GDOP is achieved:

$$\min(\text{GDOP}_{\text{TDOA}}) = \sqrt{\frac{1}{\frac{N}{4}}} = \frac{2}{\sqrt{N}}. \tag{17}$$

Proposition 2. For a TDOA positioning system with N BSs and considering the correlations between various measurements, the lowest GDOP is $2/\sqrt{N}$.

Proof. As shown above.

It is interesting that the aforementioned minimum value is identical to the minimum GDOP in the TOA positioning system [8].

The conditions for the lowest GDOP aforementioned are

$$\begin{cases} \sum_{n=1}^{N} \cos\alpha_n = 0, & \sum_{n=1}^{N} \sin\alpha_n = 0 \\ \sum_{n=1}^{N} \cos 2\alpha_n = 0, & \sum_{n=1}^{N} \sin 2\alpha_n = 0 \end{cases}. \tag{18}$$

The conclusions in (18) are consistent with those in [5] and [15], as the CRLB, FIM, and GDOP are inherently similar in nature. However, the above proof process is based on the simplified GDOP expression provided in this paper, which makes the overall approach more intuitive and concise. Further, leveraging the Euler's formula $e^{j\alpha_n} = \cos\alpha_n + j\sin\alpha_n$, the conditions can be transformed to

$$\begin{cases} \sum\limits_{n=1}^{N} e^{j\alpha_n} = 0 \\ \sum\limits_{n=1}^{N} e^{j2\alpha_n} = 0 \end{cases}. \tag{19}$$

That is, when the azimuth angles α_n of the BSs satisfy the relationship in (19), the GDOP reaches its minimum value for the number of BSs involved in the positioning.

3.3. Optimal BS Deployment Strategy for the Lowest GDOP

Inspired by the form of the sum of a complex exponential sequence in (19) the following lemma is presented:

Lemma 1. Orthogonality property of complex sinusoidal sequences. For a sequence with a general term $e^{j\frac{2\pi}{N}k(n-1)}$, we have:

$$\sum_{n=1}^{N} e^{j\frac{2\pi}{N}k(n-1)} = \frac{1-e^{j\frac{2\pi}{N}kN}}{1-e^{j\frac{2\pi}{N}k}} = \begin{cases} N, & (k = qN, q \in Z) \\ 0, & \text{otherwise} \end{cases}, \tag{20}$$

where Z denotes the set of integers.

Based on (20), $\alpha_1, \alpha_2, ..., \alpha_N$ is defined as an arithmetic sequence such that if (19) is satisfied, then the GDOP achieves its minimum value, given by

$$\alpha_n = \frac{2\pi}{N}(n-1) + \varphi, \tag{21}$$

where $\varphi \in [0, 2\pi]$ represents a bias variable.

Based on this, a proposition is derived for the optimal deployment of BSs.

Proposition 3. For a TDOA positioning system with N BSs, all BSs are allocated into M groups where $M \geq 1$, satisfying the condition $\sum_{m=1}^{M} N_m = N$, where N_m represents the number of BSs in the mth group, and $N_m \in [3, N]$. For each group, the azimuth angles of the BSs are deployed in an arithmetic progression, given by $\alpha_r^m = 2\pi(r-1)/N_m + \varphi$, where φ represents a bias variable, and $r \in [1, N_m]$. That is, all BSs involved in positioning can be divided into multiple non-overlapping groups, and the azimuths of BSs within each group are evenly distributed around a circle centered at MT. Under this configuration, the lowest GDOP is achieved.

Proof. Since $\alpha_r^m = 2\pi(r-1)/N_m + \varphi$, $\sum_{r=1}^{N_m} e^{j\alpha_r^m} = 0$ and $\sum_{r=1}^{N_m} e^{j2\alpha_r^m} = 0$ are obtained. Summing over all groups, $\sum_{m=1}^{M}\sum_{r=1}^{N_m} e^{j\alpha_r^m} = 0$ and $\sum_{m=1}^{M}\sum_{r=1}^{N_m} e^{j2\alpha_r^m} = 0$ are derived which leads to the lowest GDOP.

3.4. Uniqueness of Optimal Deployment for 3∼5 BSs

As shown in **Proposition 3**, when $N \in [3, 5]$, all BSs must be grouped together, since each group must contain at least three BSs. Building upon this, in this section, we develop a rigorous mathematical framework to prove the uniqueness of the geometric structure of the optimal BS deployment for $N \in [3, 5]$. Additionally, the non-uniqueness of the optimal deployment for $N \geq 6$ is demonstrated from a different mathematical perspective.

Lemma 2. Newton's identity. Given:

$$\begin{aligned} f(x) &= \prod_{n=1}^{N}(x - x_n) \\ &= x^N + e_1 x^{N-1} + \cdots + e_{N-1}x + e_N = 0, \end{aligned} \tag{22}$$

let

$$S_k = x_1^k + x_2^k + \cdots + x_n^k, \tag{23}$$

then we have:

$$\begin{cases} S_k + e_1 S_{k-1} + e_2 S_{k-2} + \cdots + k e_k = 0 & (1 \leq k \leq N) \\ S_k + e_1 S_{k-1} + \cdots + k e_{k-N} = 0 & (k > N) \end{cases}. \tag{24}$$

Lemma 3. Conjugate symmetry of unit complex numbers. If z is a unit complex number, then:

$$\sum\nolimits_{n=1}^{N} (1/z_n)^k = \sum\nolimits_{n=1}^{N} (\overline{z_n})^k = \overline{\sum\nolimits_{n=1}^{N} (z_n)^k}. \tag{25}$$

where $\bar{z}$ denotes the complex conjugate of z.

Construct a polynomial:

$$\begin{aligned} \prod\nolimits_{n=1}^{N}(z - z_n) &= z^N + e_1 z^{N-1} + \cdots + e_{N-1}z + e_N \\ &= 0, \end{aligned} \tag{26}$$

where $z_n = e^{j\alpha_n}$ with $|z_n| = 1$. Let $S_k = \sum_{n=1}^{N} z_n^k$. Based on **Lemma 2**, **Lemma 3**, and (19), clearly:

$$S_1 = S_2 = \overline{S_1} = \overline{S_2} = 0. \tag{27}$$

When $k = 1$ and $k = 2$ in (24), we have:

$$\begin{cases} S_1 + e_1 = 0 \\ S_2 + e_1 S_1 + 2e_2 = 0 \end{cases}. \tag{28}$$

Substituting the condition $S_1 = S_2 = 0$ into (28), we have $e_1 = e_2 = 0$. Similarly, when $k = N-2$ and $k = N-1$ in (24), according to (24), we have:

$$\begin{cases} S_{N-1} + e_1 S_{N-2} + \cdots + e_{N-3} S_2 + e_{N-2} S_1 \\ + (N-2)\, e_{N-1} = 0 \\ S_{N-2} + e_1 S_{N-3} + \cdots + e_{N-4} S_2 + e_{N-3} S_1 \\ + (N-2)\, e_{N-2} = 0 \end{cases}. \tag{29}$$

Performing the reduction in order on (26):

$$\begin{cases} z^{N-1} + e_1 z^{N-2} + \cdots + e_{N-1} + e_N / z = 0 \\ z^{N-2} + e_1 z^{N-3} + \cdots + e_{N-2} + e_{N-1}/z + e_N / z^2 = 0 \end{cases}. \tag{30}$$

Substituting all the values of z_n where n belongs to 1 to N into (30) to construct N equations. Based on **Lemma 3**, after summing all the N equations, we obtain the following two additional equations:

$$\begin{cases} S_{N-1} + e_1 S_{N-2} + \cdots + e_{N-3} S_2 + e_{N-2} S_1 \\ + N e_{N-1} + e_N \overline{S_1} = 0 \\ S_{N-2} + e_1 S_{N-3} + \cdots + e_{N-3} S_1 + N e_{N-2} \\ + e_{N-1} \overline{S_1} + e_N \overline{S_2} = 0 \end{cases}. \tag{31}$$

Comparing the structure of (29) and (31) (noting the coefficients of e_{N-1} and e_{N-2}) and considering that $\overline{S_1} = \overline{S_2} = 0$, (29) and (31) will only hold simultaneously when $e_{N-2} = e_{N-1} = 0$. In conclusion, we have:

$$e_1 = e_2 = e_{N-2} = e_{N-1} = 0. \tag{32}$$

Therefore, (26) can be simplified to:

$$z^N + e_3 z^{N-3} + \cdots + e_{N-3} z^3 + e_N = 0. \tag{33}$$

For the case of $N \in [3, 5]$, (33) can be directly simplified to:

$$z^N = -e_N. \tag{34}$$

Considering the case where $|z_n| = 1$ and solving (34), we get:

$$z_n = e^{j\alpha_n} = \sqrt[N]{-e_N} = e^{j(\varphi + 2(n-1)\pi/N)} \quad (n = 1, 2, \cdots, N), \tag{35}$$

which confirms the uniqueness of (21) for $N \in [3, 5]$.

For the case of $N \geq 6$, due to the uncertainty of e_3 to e_{N-3}, (21) is not the unique optimal geometric structure of the deployment which confirms the existence of the BS grouping situation as described in **Proposition 3**.

Proposition 4. For a TDOA positioning system with N BSs and considering the correlations between various measurements, the geometric configuration for optimal BS deployment exhibits uniqueness for up to five BSs. However, non-uniqueness arises when the number of BSs exceeds five.

Proof. As shown above.

3.5. The Highest GDOP Value and Its Conditions

Notably, under the condition that all azimuths are not identical (note that, as stated in Section 3.2, when the azimuths are identical, the GDOP becomes undefined), setting the denominator of (11) to zero results in an infinite GDOP value.

Proposition 5. For a TDOA positioning system with N BSs and considering the correlations between various measurements, the highest GDOP is infinite.

Proof. As shown above.

Note that $AB = C^2$ leads to the denominator of (11) equaling 0. According to the Cauchy-Schwarz inequality in probability theory:

$$\mathrm{var}(a_n)\mathrm{var}(b_n) \geq \mathrm{cov}^2(a_n, b_n), \tag{36}$$

i.e.,

$$AB \geq C^2. \tag{37}$$

From the mathematical structure of (37), the first condition for equality can be derived: $A = 0$ or $B = 0$, i.e.,

$$\begin{cases} \cos\alpha_1 = \cos\alpha_2 = \cdots = \cos\alpha_N \\ \sin\alpha_1 = \sin\alpha_2 = \cdots = \sin\alpha_N \end{cases}, \tag{38}$$

when one of the conditions in (38) holds, equality in (37) is satisfied. From the equality condition of the Cauchy-Schwarz inequality in probability theory, the second condition for equality in (37) can be derived: when $\cos\alpha_n$ and $\sin\alpha_n$ are linearly related, which means that there exists a scalar λ such that $\sin\alpha_n = \lambda\cos\alpha_n$, equality holds in (37). In this case, $\lambda = \tan\alpha_n$, i.e., when

$$\tan\alpha_1 = \tan\alpha_2 = \cdots = \tan\alpha_N, \tag{39}$$

equality in (37) is satisfied. In conclusion, we have:

$$\begin{cases} \cos\alpha_1 = \cos\alpha_2 = \cdots = \cos\alpha_N \\ \sin\alpha_1 = \sin\alpha_2 = \cdots = \sin\alpha_N \\ \tan\alpha_1 = \tan\alpha_2 = \cdots = \tan\alpha_N \end{cases}, \tag{40}$$

when one of the conditions in (40) holds, the GDOP reaches its maximum value of infinity. It is important to note that when both the first and second conditions hold simultaneously, the GDOP becomes undefined, resulting in a $0/0$ degenerate case.

3.6. Worst-Case BS Deployment Strategy for the Highest GDOP

If one of the conditions in (40) is satisfied, considering the periodicity of the trigonometric functions and the fact that $\alpha_n \in [0, 2\pi]$, the azimuths of the BSs have exactly two possible values. In conclusion:

$$\alpha_n \in \{\beta_1, \beta_2\}, \quad (|\beta_1 - \beta_2| = \pi \text{ or } \beta_1 + \beta_2 = k\pi,\ k \in \{1, 2, 3\}). \tag{41}$$

When the condition in (41) is satisfied, the GDOP reaches its maximum value of infinity. This represents the complete solution set for the worst-case BS deployment strategy.

Proposition 6. For a TDOA positioning system with N BSs, the highest GDOP is achieved when the azimuths of all BSs have exactly two distinct values which satisfy the conditions in (41).

Proof. As shown above.

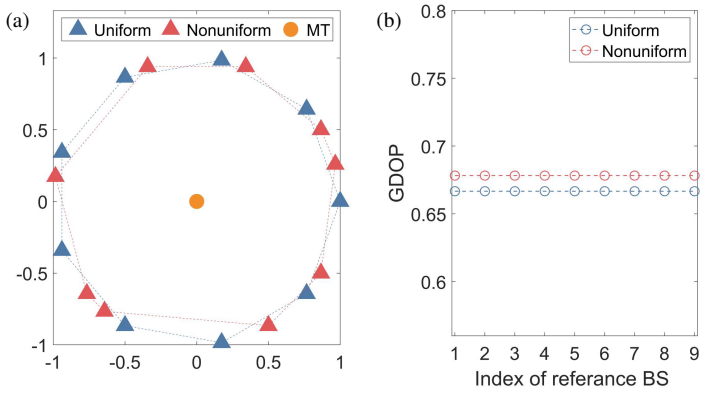

FIGURE 2. BSs deployment and GDOP performance for the case with $N = 9$. (a) Geometry. (b) GDOP curves under various reference BSs.

4. SIMULATION RESULTS

The simulation results in this section are divided into two parts: the first part presents various TDOA positioning scenarios designed to validate the propositions put forward in this paper. The second part discusses the applicability of the optimal deployment strategy proposed in **Proposition 3** to other positioning methods, including TOA and DOA. Additionally, the GDOP results from the proposed method are compared with those using the approximation in [9], showing consistently lower values with our approach.

TABLE 1. Results of GDOP bounds using IPM.

N	Lower bound	Upper bound
3	1.154700538	8911830.227
4	1.000000000	316549.8981
5	0.894427191	1061.704283
6	0.816496581	1248.882994
7	0.755928946	16617.44445
8	0.707106781	2955691.221
9	0.666666667	61640.35274

4.1. Validation of the Propositions

A two-dimensional TDOA positioning scenario involving multiple BSs and one MT is considered for performance analysis, where the MT is located at the origin. From (7), it is evident that the GDOP is solely determined by the azimuthal angles of the BSs and is independent of the distances between the BSs and MT. For simplicity, we assume equal distances between the MT and all BSs, with the BSs deployed on a unit circle.

The analysis begins with $N = 9$ BSs. Two cases are considered: uniform and nonuniform, as shown in Fig. 2(a), respectively. Each BS is selected in turn as the reference BS, and the corresponding GDOP is recorded. The flat curves in Fig. 2(b) confirm that the choice of reference BS does not affect the GDOP, in accordance with **Proposition 1**. Additionally, the GDOP values for the uniform deployment are lower than those for nonuniform deployment.

Also, multiple test cases are designed by varying N from 3 to 9 to validate the GDOP bounds announced in this paper. The interior-point method (IPM) [17], an effective approach for solving optimization problems with multiple variables, is selected for BS assignment and used for comparison. In such a method, we set (7) as the fitness function and aim to optimize it to its minimum value. The azimuths of the BSs, denoted as α_n, are treated as a set of optimization variables (with a total of N variables), where the lower bound of all optimization variables is 0, and the upper bound is 2π. The results are presented in Table 1. For the GDOP lower bound, it is observed that for each N, the lowest GDOP value is almost identical to the expression $2/\sqrt{N}$, which corresponds to **Proposition 2**. Moreover, the lowest GDOP value decreases as the number of BSs increases. For the GDOP upper bound, it is observed that the highest GDOP results of the IPM are very large, although they do not approach infinity value in **Proposition 5**.

For the BS deployment pattern, the simulation primarily focuses on visualization. It starts with the optimal deployment. The test case with $N = 11$ BSs is modeled to evaluate the proposed deployment strategy in **Proposition 3**. Five strategies, denoted as S_1, S_2, S_3, S_4, and S_5 are defined, with all BSs distributed into various groups. For each group, the azimuth angles of the BSs follow an arithmetic progression, meaning that the positions of all BSs form a regular polygon. All these strategies satisfy the conditions in **Proposition 3**, thereby ensuring that (7) reaches its minimum value under the condition of $N = 11$. Fig. 3 and Table 2 illustrate the definitions of these strategies. Take S_4 for instance, the $N = 11$ BSs are divided into $M = 3$ groups, with each group containing $N_m = 3, 3, 5$ BSs, respectively, arranged in the shape of regular polygons. The bias variables in (21) for each group are $\varphi = 0.7505, 1.5359, 1.1868$, respectively. The azimuth angles of the BSs for each strategy are substituted into (7), yielding the corresponding GDOP values, which are recorded in the fourth column of Table 2. Clearly, the GDOP values for all strategies are equal and correspond to the lower bound value of $2/\sqrt{11}$, as they all satisfy the conditions in **Proposition 3**, namely, in each strategy, the $N = 11$ BSs can be divided into one, two, or three groups (with no overlap between BSs in each group), and the azimuths of the BSs within each group follow a uni-

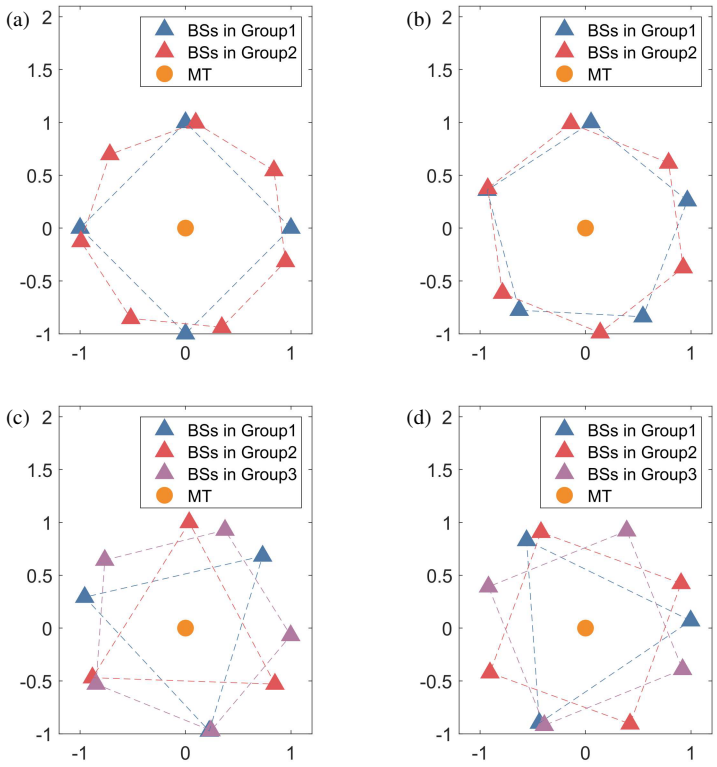

FIGURE 3. BSs deployment for the case with $N = 11$. (a) S_2, (b) S_3, (c) S_4, (d) S_5.

TABLE 2. Definitions and performance of five strategies.

Strategy	Assignment	M	GDOP
S_1	Group 1: Regular 11-gon ($\varphi = 0.0000$)	1	0.603022689
S_2	Group 1: Regular 4-gon ($\varphi = 0.0000$) Group 2: Regular 7-gon ($\varphi = 0.5756$)	2	0.603022689
S_3	Group 1: Regular 5-gon ($\varphi = 0.2618$) Group 2: Regular 6-gon ($\varphi = 0.6632$)	2	0.603022689
S_4	Group 1: Regular 3-gon ($\varphi = 0.7505$) Group 2: Regular 3-gon ($\varphi = 1.5359$) Group 3: Regular 5-gon ($\varphi = 1.1868$)	3	0.603022689
S_5	Group 1: Regular 3-gon ($\varphi = 0.0698$) Group 2: Regular 4-gon ($\varphi = 0.4363$) Group 3: Regular 4-gon ($\varphi = 1.1694$)	3	0.603022689

form distribution. Additionally, Fig. 4 illustrates the example of each possible scenario in the worst-case deployment solution set, as presented in **Proposition 6**, where the GDOP value for each geometric structure is infinite.

4.2. Generalization of the Propositions

To explore the broader applicability of the proposed BSs deployment method, we investigate its performance in two-dimensional TOA and DOA systems. According to [7], the GDOP in two-dimensional TOA and DOA can be expressed as:

$$\mathrm{GDOP}_{\mathrm{TOA}} = \sqrt{\frac{N}{\sum_{i=1}^{N-1}\sum_{j=i+1}^{N}\sin^2(\alpha_j - \alpha_i)}}, \tag{42}$$

$$\mathrm{GDOP}_{\mathrm{DOA}} = \sqrt{\frac{\sum_{i=1}^{N} d_i^{-2}}{\sum_{i=1}^{N-1}\sum_{j=i+1}^{N} d_i^{-2} d_j^{-2}\sin^2(\alpha_j - \alpha_i)}}. \tag{43}$$

It is observed that the GDOP for TOA is independent of the distances between the BSs and MT, whereas the GDOP for DOA is distance-dependent. Notably, when the BS-MT distances in

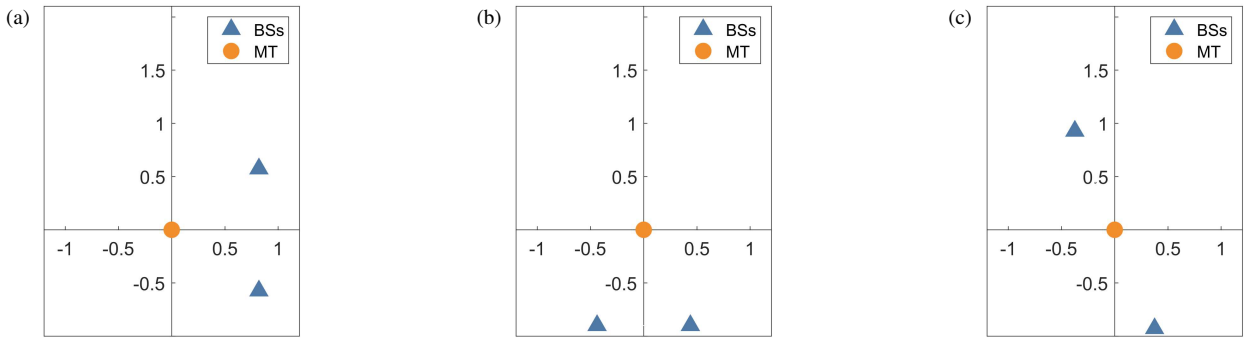

FIGURE 4. Complete solution set for the worst-case BS deployment strategy for highest GDOP. (a) Horizontal axis symmetry of BSs. (b) Vertical axis symmetry of BSs. (c) Origin symmetry of BSs.

TABLE 3. Results of GDOP values for TOA and DOA.

Strategy	TOA-1	DOA-1	DOA-2	DOA-IPM
S_1	0.603022689	0.603022689	1.405652504	
S_2	0.603022689	0.603022689	1.315183222	
S_3	0.603022689	0.603022689	1.431289438	1.312499128
S_4	0.603022689	0.603022689	1.534209137	
S_5	0.603022689	0.603022689	1.462450071	

DOA are equal, the GDOP for DOA is simplified to the GDOP for TOA multiplied by the distance between the BS and MT. In order to conduct a more comprehensive evaluation, we designed four test cases to calculate the GDOP: TOA-1, DOA-1, DOA-2, DOA-IPM. TOA-1 is based on the TOA positioning method, and DOA-1, DOA-2, and DOA-IPM are based on DOA positioning method. In both TOA-1 and DOA-1 cases, the GDOP for the five strategies S_1, S_2, S_3, S_4, and S_5 is directly calculated under their respective positioning methods. In DOA-2 case, for each of the five strategies S_1–S_5, the azimuth angles of each BS remain consistent with Table 2, while the distances between BS and MT are assigned new values. Specifically, for each strategy, distances vector $\mathbf{d}_{\text{DOA-2}}$ is defined to record BS-MT distances where $\mathbf{d}_{\text{DOA-2}} = [8.1472, 9.0579, 1.2699, 9.1338, 6.3236, 0.9754, 2.7850, 5.4688, 9.5751, 9.6489, 1.5761]$, i.e., for each strategy, the distance between the nth BS and MT d_n is equal to the $\mathbf{d}^{(n)}_{\text{DOA-2}}$, where $\mathbf{d}^{(n)}_{\text{DOA-2}}$ refers to the nth element of the vector $\mathbf{d}_{\text{DOA-2}}$. Then, the GDOP values for strategies S_1–S_5 are calculated under DOA method. In DOA-IPM case, we utilize the IPM to optimize the GDOP under the DOA positioning method. We select (43) as the fitness function with the goal of minimizing it. For comparison with DOA-2, the BS-MT distances in this case are taken from the values in $\mathbf{d}_{\text{DOA-2}}$ and are used as constants in the fitness function. The azimuths of the BSs α_n are treated as a set of optimization variables (with a total of $N = 11$ variables), where the lower bound of all optimization variables is 0, and the upper bound is 2π. The results for TOA-1, DOA-1, DOA-2, and DOA-IPM are recorded in Table 3. It is first observed that the GDOP in TOA-1 reaches its minimum value $2/\sqrt{N}$ reported in [8]. Simultaneously, the GDOP in DOA-1 is equal to those in TOA-1. This equivalence arises because, in these five strategies S_1–S_5, the distances between all BSs and MTs are preset to 1 (with the MT located at the origin and the BSs deployed on a unit circle). This geometric configuration results in the equality of (42) and (43). Consequently, the GDOP for DOA-1 also achieves its minimum value. Furthermore, we observe that the GDOP values for the five strategies under the DOA-2 configuration differ and consistently exceed the GDOP result obtained with DOA-IPM, indicating that the minimum value is not attained. Collectively, these results demonstrate that the optimal deployment strategy proposed in **Proposition 3** for the TDOA system is also applicable to both TOA and DOA systems with equal BS-MT distances. However, this strategy does not apply to DOA positioning systems characterized by unequal BS-MT distances.

Additionally, for the TDOA scenario, we compare the proposed CRLB-based GDOP estimation method with the LS-based GDOP approximation. The comparison involves strategies S_1, S_2, S_3, S_4, and S_5 under equal BS-MT distances condition (with the MT located at the origin and the BSs deployed on a unit circle). For the LS-based approximation, considering the unit distance 1 between BSs and MT, we assume that the variance of all TDOA measurements is 0.001 to simulate a 30 dB signal-to-noise ratio (SNR) environment. Furthermore, to align with the dimensionless GDOP metric used in our proposed method, we normalize the LS-based GDOP results by dividing them by the standard deviation of this variance. Each strategy (S_1–S_5) is evaluated over 1000 independent trials, with average results recorded in Table 4. It is observed that the LS-based GDOP values vary across different strategies and are consistently higher than the CRLB-based GDOP values. This indicates that the LS estimation method for expressing GDOP is inaccurate, demonstrating that the CRLB-based GDOP pro-

TABLE 4. Results of GDOP using different methods.

Strategy	CRLB-based GDOP	LS-based GDOP
S_1	0.603022689	0.839196935
S_2	0.603022689	0.796717028
S_3	0.603022689	0.810481415
S_4	0.603022689	0.823699297
S_5	0.603022689	0.820328505

vides a more reliable metric for evaluating positioning accuracy across diverse deployment strategies.

5. CONCLUSION

This work investigates the GDOP bounds and the corresponding BS deployment for two-dimensional TDOA-based positioning systems. The analysis confirms that the uniform angular distribution of BSs groups around the MT minimizes GDOP. For systems with three to five BSs, polynomial root analysis proves the uniqueness of the optimal deployment, while configurations with six or more BSs admit multiple valid solutions due to increased geometric flexibility. The complete solution set for worst-case deployment, characterized by collinear or angularly clustered BSs, induces infinite GDOP through geometric degeneracy. Key advancements include a simplified GDOP formulation, the invariance of GDOP to reference BS selection, and a theoretical framework integrating complex number theory and algebraic theory with GDOP bounds and BS deployment analysis. Numerical simulations validate the theoretical findings for the two-dimensional TDOA system and investigate the applicability of the proposed BS deployment strategy to other positioning systems, including two-dimensional TOA and DOA. Future research may extend this work to three-dimensional environments. The proposed methodology extends the classical understanding of GDOP and offers theoretical insights for designing high-accuracy cellular positioning systems.

REFERENCES

[1] Khalife, J. and Z. M. Kassas, "Differential framework for submeter-accurate vehicular navigation with cellular signals," *IEEE Transactions on Intelligent Vehicles*, Vol. 8, No. 1, 732–744, Jan. 2023.

[2] Gabber, E. and A. Wool, "On location-restricted services," *IEEE Network*, Vol. 13, No. 6, 44–52, Nov.–Dec. 1999.

[3] Coronado, A. E., C. S. Lalwani, E. S. Coronado, and S. Cherkaoui, "Wireless vehicular networks to support road haulage and port operations in a multimodal logistics environment," in *2008 IEEE International Conference on Service Operations and Logistics, and Informatics*, 550–555, Beijing, China, 2008.

[4] Abd El-Haleem, A. M., M. G. Anany, A. I. Salama, G. A. Khalaf, and M. M. Elmesalawy, "Violation detection technique for COVID-19 self-isolation and control measures using wireless and geofencing technologies," in *2022 International Conference on Electronics, Information, and Communication (ICEIC)*, 1–6, Jeju, Republic of Korea, 2022.

[5] Lui, K. W. K. and H.-C. So, "A study of two-dimensional sensor placement using time-difference-of-arrival measurements," *Digital Signal Processing*, Vol. 19, No. 4, 650–659, Jan. 2009.

[6] Sharp, I., K. Yu, and Y. J. Guo, "GDOP analysis for positioning system design," *IEEE Transactions on Vehicular Technology*, Vol. 58, No. 7, 3371–3382, Sep. 2009.

[7] Shi, W., X. Qi, J. Li, S. Yan, L. Chen, Y. Yu, and X. Feng, "Simple solution to the optimal deployment of cooperative nodes in two-dimensional TOA-based and AOA-based localization system," *EURASIP Journal on Wireless Communications and Networking*, Vol. 2017, No. 1, 79, Apr. 2017.

[8] Levanon, N., "Lowest GDOP in 2-D scenarios," *IEE Proceedings — Radar, Sonar and Navigation*, Vol. 147, No. 3, 149–155, Jun. 2000.

[9] Mahyuddin, M. F. M., A. A. M. Isa, and N. Hassan, "Optimal station distribution for closed form TDOA measurement," *Journal of Theoretical and Applied Information Technology*, Vol. 98, No. 11, 1842–1853, Jun. 2020.

[10] Li, W., P. Wei, and X. Xiao, "A robust TDOA-based location method and its performance analysis," *Science in China Series F: Information Sciences*, Vol. 52, No. 5, 876–882, May 2009.

[11] Deng, Z., H. Wang, X. Zheng, and L. Yin, "Base station selection for hybrid TDOA/RTT/DOA positioning in mixed LOS/NLOS environment," *Sensors*, Vol. 20, No. 15, 4132, 2020.

[12] Deng, Z., H. Wang, X. Zheng, X. Fu, L. Yin, S. Tang, and F. Yang, "A closed-form localization algorithm and GDOP analysis for multiple TDOAs and single TOA based hybrid positioning," *Applied Sciences*, Vol. 9, No. 22, 4935, Nov. 2019.

[13] Deng, P. and L. Yu, "GDOP performance analyze of cellular location system," *Journal of Southwest Jiaotong University*, Vol. 40, No. 2, 185–188, Apr. 2005.

[14] Liu, Z. and S. Lin, "Optimal base station deployment of TDOA-based positioning system," in *2021 IEEE USNC-URSI Radio Science Meeting (Joint with AP-S Symposium)*, 108–109, Singapore, 2021.

[15] Wang, W., P. Bai, Y. Wang, X. Liang, and J. Zhang, "Optimal sensor deployment and velocity configuration with hybrid TDOA and FDOA measurements," *IEEE Access*, Vol. 7, 109 181–109 194, 2019.

[16] Torrieri, D. J., "Statistical theory of passive location systems," *IEEE Transactions on Aerospace and Electronic Systems*, Vol. 20, No. 2, 183–198, Mar. 1984.

[17] Lin, Z., D. Zhu, and Z. Sheng, "Finding a minimal efficient solution of a convex multiobjective program," *Journal of Optimization Theory and Applications*, Vol. 118, No. 3, 587–600, Sep. 2003.